Spontaneous Intracerebral Hematoma on Diffusion-weighted Images: Influence of T2-shine-through and T2-blackout Effects

Stéphane Silvera, Catherine Oppenheim, Emmanuel Touzé, Denis Ducreux, Philippe Page, Valérie Domigo, Jean-Louis Mas, François-Xavier Roux, Daniel Frédy and Jean-François Meder

AJNR Am J Neuroradiol 2005, 26 (2) 236-241
http://www.ajnr.org/content/26/2/236

AJNR Am J Neuroradiol 26:236–241, February 2005

Spontaneous Intracerebral Hematoma on Diffusion-weighted Images: Influence of T2-shine-through and T2-blackout Effects

Stéphane Silvera, Catherine Oppenheim, Emmanuel Touzé, Denis Ducreux, Philippe Page, Valérie Domigo, Jean-Louis Mas, François-Xavier Roux, Daniel Frédy, and Jean-François Meder

BACKGROUND AND PURPOSE: **On diffusion-weighted (DW) images, primary hematomas are initially mainly hyperintense, and then hypointense during the first few days after stroke onset. As in other brain disorders, variations in the T2 relaxation time of the hematoma influence the DW imaging signal intensity. Our aim was to evaluate the contribution of the T2 signal intensity and apparent diffusion coefficient (ADC) changes to signal intensity displayed by DW imaging through the course of hematoma.**

METHODS: **The MR images of 33 patients with primary intracranial hemorrhage were retrospectively reviewed. Variations in T2-weighted echo planar images, DW imaging signal intensity, and apparent diffusion coefficient (ADC) ratios (core of hematoma/contralateral hemisphere) were analyzed according to the putative stages of hematoma, as seen on T1- and T2-weighted images.**

RESULTS: **On both T2-weighted echo planar and DW images, the core of the hematomas was hyperintense at the hyperacute (oxyhemoglobin, $n = 11$) and late subacute stages (extracellular methemoglobin, $n = 4$), while being hypointense at the acute (deoxyhemoglobin, $n = 11$) and early subacute stages (extracellular methemoglobin, $n = 7$). There was a positive correlation between the signal intensity ratio on T2-weighted echo planar and DW images ($r = 0.93$, $P < .05$). ADC ratios were significantly decreased in the whole population and in each of the first three stages of hematoma, without any correlation between DW imaging findings and ADC changes ($r = 0.09$, $P = .6$).**

CONCLUSION: **Our results confirm that the core of hematomas is hyperintense on DW images with decreased ADC values at the earliest time point, and may thus mimic arterial stroke on DW images. T2 shine-through and T2 blackout effects contribute to the DW imaging findings of hyperintense and hypointense hematomas, respectively, while ADC values are moderately but consistently decreased during the first three stages of hematoma.**

MR imaging is increasingly used for the initial emergent examination of patients presenting with sudden neurologic symptoms owing to the high sensitivity of diffusion-weighted (DW) imaging for the detection of ischemic brain damage. Primary intracerebral hemorrhage is responsible for up to 15% of all strokes and is associated with a high rate of mortality (1). There is a body of literature (2–5) supporting the use of MR imaging as the only technique for imaging patients with acute stroke. In this setting, identification of the intracranial hemorrhage by using MR imaging is critical to the determination of appropriate stroke management. On conventional MR images, the signal intensity of the hematoma is relatively complex and has been extensively studied (6–12). The signal intensity of blood products typically changes over time, as extravasated red blood cells degrade, resulting in predictable imaging patterns on T1-, T2-, and T2*-weighted MR images. As DW imaging now plays a crucial role in the evaluation of acute stroke, it becomes paramount to characterize hematoma on the basis of DW imaging findings (13–17). In a first study, Atlas et al (13) reported that restricted diffusion (i.e., low apparent diffusion coefficient [ADC]) was present in early hematoma containing intact red blood cell membranes and increased diffusion when

Received February 27, 2004; accepted after revision July, 6.

From the Departments of Neuroradiology (S.S., C.O., D.D., D.F., J.-F.M.), Neurology (E.T., V.D., J.-L.M.), and Neurosurgery (P.P., F.-X.R.), Centre Hospitalier Sainte-Anne, Université Paris V, Paris, France.

Address reprint requests to Dr. Catherine Oppenheim, Département d'Imagerie Morphologique et Fonctionnelle, Centre Hospitalier Sainte-Anne, 1 rue Cabanis, 75674 Paris cedex 14, France, oppenheim@chsa.broca.inserm.fr.

red cell membranes had lysed. The latter result was contested by others (16) who reported decreased ADC even at the stage of extracellular methemoglobin. Most hematomas are initially hyperintense on DW images, and then hypointense during the first few days after onset, as shown qualitatively by other groups (13, 16). It has been suggested that variations in the T2 relaxation time of a hematoma may affect the signal intensity displayed by DW imaging (16, 17). To test this hypothesis, we simultaneously analyzed the T2-weighted echo planar and DW imaging signal intensity variations and ADC changes throughout the course of the hematoma.

Methods

Patients

Among all consecutive patients admitted to our institution between June 2001 and August 2003, we retrospectively selected those who fulfilled the following criteria: 1) sudden onset of acute neurologic symptoms due to an intracerebral hematoma; 2) MR imaging including DW imaging; and 3) absence of underlying tumor, arterial or venous stroke, traumatic injury, or large arteriovenous malformation on initial clinico-radiologic and follow-up examination, since these might produce ADC changes. Thirty-three patients (12 women and 21 men; mean age, 56 years; range, 19–83) fulfilled these criteria and constituted our study group. The median delay from clinical onset to MR imaging was 27 hours (minimum = 2 hours; maximum = 10 days). When a patient underwent sequential MR imaging, only the initial examination was considered for this study. Hematomas were presumed to be due to hypertension in 16 cases, anticoagulation treatment in six cases, and small arteriovenous malformation or aneurysm in four cases. The cause of stroke remained unknown in seven cases, three of which after digitized angiography.

MR Imaging

MR imaging was performed on a 1.5T system (1.5T Signa Echospeed scanner, GE Medical Systems, Milwaukee, WI) including at least the following three sequences: 1) axial or sagittal T1-weighted sequence; 2) axial fast fluid-attenuated inversion recovery sequence (matrix, 256 × 192; FOV, 24 × 24 cm; [TR/TE_{eff}/TI], 9800/152/2300 ms; section thickness, 6 mm; imaging time, 3.17 minutes); 3) axial T2-weighted baseline acquisition ($b = 0$ s/mm^2), and DW imaging were acquired with a single shot echo planar spin-echo sequence (matrix, 128 × 128; FOV, 24 × 24 cm; 5000/88 ms [TR/TE_{eff}]). The diffusion trace images were calculated from three diffusion-weighted acquisitions with the diffusion gradients sequentially applied along each of the three orthogonal axes, with $b = 1000$ s/mm^2, $\delta = 32$ ms, $\Delta = 39$ ms and G = 22 mT/m. All axial images were acquired by using a 6-mm section thickness, no gap, and 20 sections enabling whole-brain coverage. Trace images were generated and ADC maps calculated with a dedicated software tool, without masking for background noise on T2-weighted baseline images ($b = 0$ s/mm^2) (Functool, General Electric, Buc, France).

Image Analysis

Hematomas were qualitatively analyzed according to the putative stages of brain hematoma, as determined from T1- and T2-weighted pulse sequences, and classified into four groups (intracellular oxyhemoglobin, intracellular deoxyhemoglobin, intracellular and extracellular methemoglobin) (8). Because hematomas usually display a combination of blood products, this grouping was made on the basis of the major component, as determined from the signal intensities on T1- and T2-weighted pulse sequences. There were 11 hematomas at the oxyhemoglobin stage (delay to MR imaging = 8 ± 8 hours, mean ± SD), 11 at the deoxyhemoglobin stage (delay to MR imaging = 47 ± 30 hours), seven at the methemoglobin intracellular stage (delay to MR imaging = 63 ± 40 hours), and four at the methemoglobin extracellular stage (delay to MR imaging = 85 ± 103 hours). Thirty-one hematomas were supratentorial and the two others were infratentorial. Hematomas were lobar in 13 patients, located in the basal ganglia in 18 patients, and in the cerebellar vermis in two patients.

For each patient, the section on which the hematoma was the largest and surrounded by a hypointense ring on the echo planar T2-weighted echo-planar image ($b = 0$ s/mm^2) was selected and used for all following measurements (Fig 1). The manual contouring of the hematoma was performed on T2-weighted images because of its sensitivity to the susceptibility magnetic effects and the similarity of spatial echo planar image distortions with those of DW imaging (14, 15, 18). The outer limit of the region of interest corresponded to the external limit of the T2-hypointense ring, with care taken to avoid the T2-hyperintense edema surrounding the core of the hematoma. In one case, the hypointense ring was not clearly visible on the echo planar T2-weighted image, and the entire area of hyperintensity was contoured. Regions of interest were mirrored onto the uninvolved contralateral hemisphere. For each hematoma, the signal intensity was visually graded as hyper-, iso-, or hypointense relative to the contralateral parenchyma on T2-weighted echo planar and DW images acquired at each stage of the hematoma. S_{T2} and S_{DW} corresponded to the average signal intensity of the hematoma measured in arbitrary values on T2-weighted echo planar and DW images, respectively. rS_{DW} and rS_{T2} corresponded to the signal intensity ratio (ipsilateral/contralateral) measured on DW and T2-weighted echo planar images, respectively. ADC, mirADC, and rADC corresponded to the mean absolute ADC values in the core of the hematoma, the mirror region of interest, and the ratio of these mean ADC values.

Statistical Analysis

S_{DW} and S_{T2} at each evolving stage of hematoma were compared with $mirS_{DW}$ and $mirS_{T2}$, respectively, by using a paired non-parametric Wilcoxon test. The relationship between rS_{T2}, rADC, and rS_{DW} was tested by using a Pearson correlation test. ADC was compared with mirADC in the whole population and in each subgroup of hematoma by using a paired non-parametric Wilcoxon test. Since the hypothesis of intraclass equality of variances was not satisfied, we used the Kruskal-Wallis rank test to look for differences in rS_{DW}, rS_{T2}, and rADC values between the four hemorrhagic stages. The level of significance was set at $P < .05$.

Results

As illustrated in Figure 2, the core of hyperacute ($n = 11$) and late subacute ($n = 4$) hematomas was hyperintense, while acute ($n = 11$) and early subacute ($n = 7$) hematomas were hypointense relative to the normal-appearing brain parenchyma on both DW and T2-weighted echo planar images. Signal intensity ratios varied significantly between stages on DW ($P < .001$) and T2-weighted echo planar images ($P < .01$). Accordingly, rS_{DW} and rS_{T2} were significantly increased at the hyperacute stage (rS_{DW}: $P = .007$; rS_{T2}: $P = .01$), while these ratios were significantly decreased at the acute (rS_{DW}: $P = .004$; rS_{T2}: $P = .003$) and early subacute stages (rS_{DW}: $P = .03$; rS_{T2}: $P = .02$). Significance was not reached for rS_{DW} or rS_{T2} in

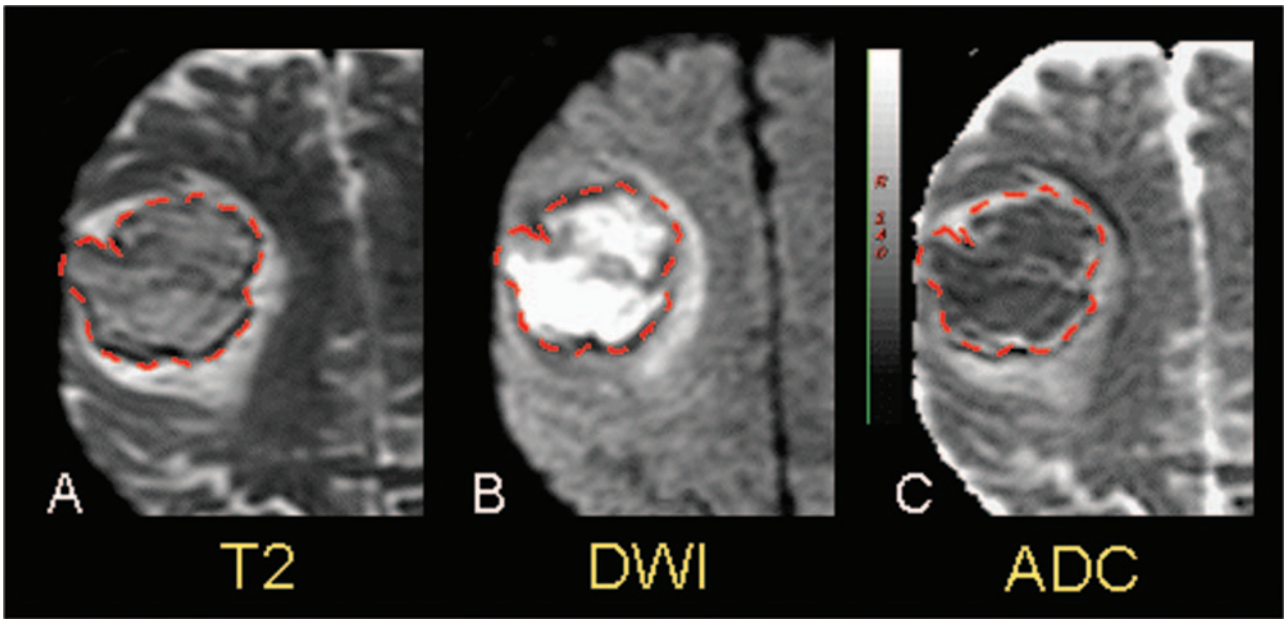

FIG 1. Manual contouring of the hematoma.

A, On the T2-weighted echo planar image (b = 0 mm^2/s) on which the hematoma appears largest, the outer limit of the region of interest corresponded to the T2-hypointense ring.

B, The region of interest is copied on the diffusion-weighted image (b = 1000 mm^2/s).

C, Mean absolute ADC values are computed in the region of interest. Mirror region of interest is placed on the contralateral hemisphere to compute the rADC.

the late subacute group (n = 4). There was a significant positive correlation between rS_{DW} and rS_{T2} (r = 0.93, $P < .05$) for the whole population, which remained significant when T2-hyperintense (r = 0.76, $P < .05$) and T2-hypointense (r = 0.92, $P < .05$) hematomas were analyzed separately (Fig 3). In the whole population, the ADC was significantly decreased when compared with the mirADC ($P < .001$). This remained significant within each subgroup, except in the late subacute group (P = .06). Mean absolute ADC values were 695 $\times$ 10^{-6} mm^2/s at the hyperacute stage, 713 $\times$ 10^{-6} mm^2/s at the acute stage, 740 $\times$ 10^{-6} mm^2/s at the early subacute stage, and 677 $\times$ 10^{-6} mm^2/s at the late subacute stage. rADCs were 0.81 at the hyperacute stage, 0.82 at the acute stage, 0.82 at the early subacute stage, and 0.76 at the late subacute stage (Fig 4), without any significant difference in the rADC between all four stages (P = .89, 3° of freedom). No correlation existed between rADC and rS_{DW} (r = 0.09, P = .6).

Discussion

Several studies have suggested that MR imaging is a reliable screening method for primary intraparenchymal hemorrhage (2–5, 7) and have documented the patterns of evolving hematoma on conventional MR images. These MR imaging patterns remain somewhat complex and are further complicated by the advent of new MR imaging techniques, such as DW imaging. Although DW imaging is probably not the key sequence for the diagnosis of intraparenchymal hematoma, it is mandatory to further our understanding of the signal intensity variations of primary hematomas on the basis of DW imaging findings to reduce the risk of misdiagnosis. Among factors that contribute to the DW imaging signal intensity changes of a hematoma over time, the restriction of diffusion and the level of T2 signal intensity changes may play an important role (13, 16, 17). To assess these hypotheses, we simultaneously analyzed the T2- and DW imaging signal intensity variations and ADC changes in the evolving hematoma. Our quantitative analysis showed that similar signal intensity changes were observed on DW and T2-weighted echo planar images throughout the course of the hematoma, while ADC values were uniformly lowered at all four stages of hematoma.

Other investigators have recognized that the hematoma signal intensity on DW images varies with time (4, 16, 17), but have not thoroughly quantified these signal intensity changes. We quantitatively confirm that, at the hyperacute stage, the core of the hematoma is mainly hyperintense on DW images. Evolution into "acute" hematoma, when oxygenated hemoglobin turns into deoxygenated hemoglobin, is identified as a marked hypointense core on DW images (17). This low DW imaging signal intensity has been shown to persist at the early subacute stage, while late subacute hematoma displays DW imaging hyperintensity (13, 16, 17).

Further analysis of our data indicated that the ADC values of hematomas (including hyperacute, acute, and early subacute stages) were moderately but significantly reduced compared with those of the contralateral, normal brain parenchyma. These data strengthen the main findings of Atlas et al (13), as well as those of other groups (15, 16), who showed

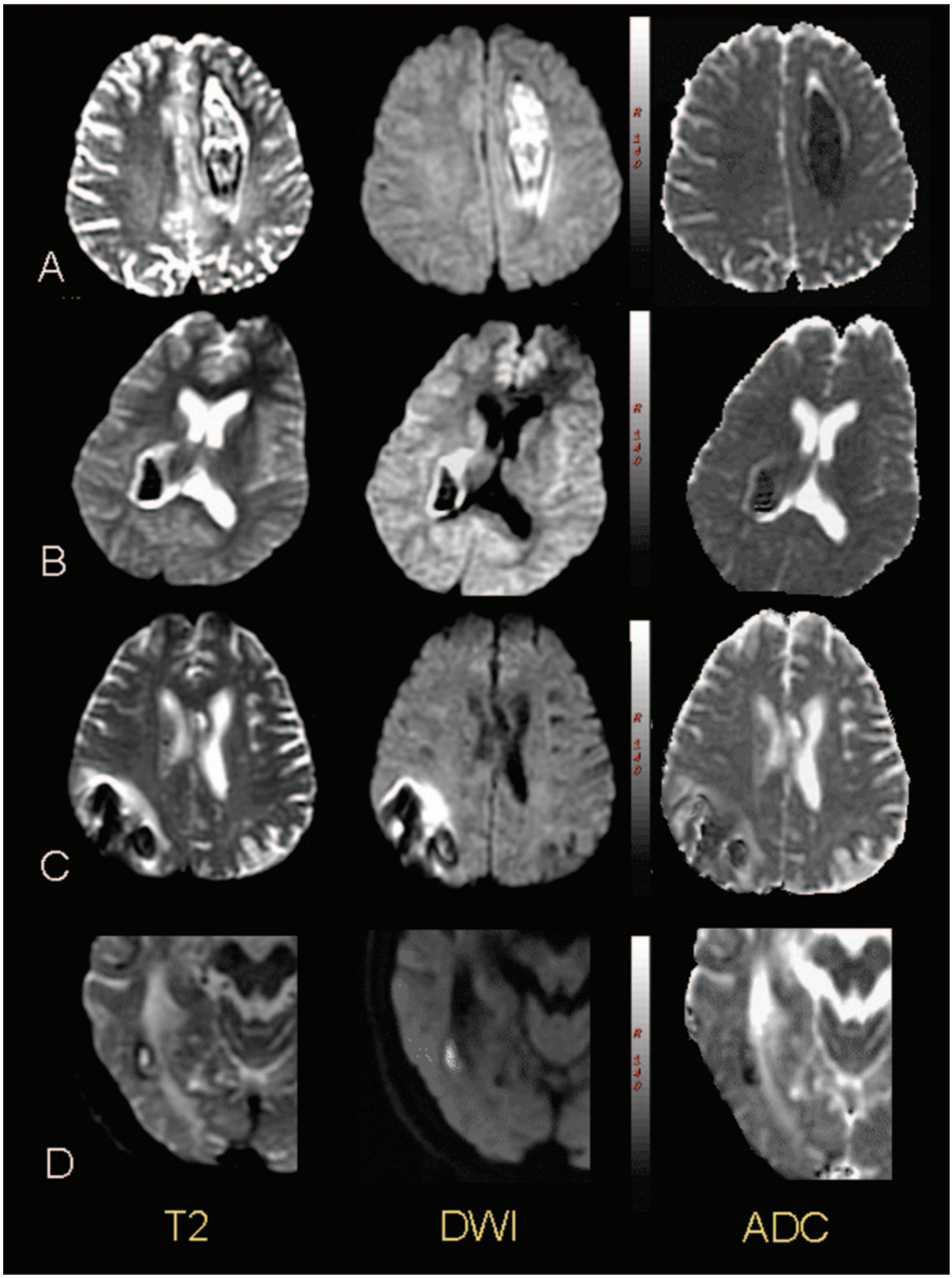

FIG 2. T2 shine-through (A, D) and T2 blackout effects (B, C) in intracerebral hematomas.

A, Hyperacute hematoma in a 28-year-old man. The frontal lobe hematoma is isointense on a T1-weighted, hyperintense on a fluid-attenuated inversion recovery (not shown), T2-weighted, and DW image acquired with low ADC values.

B, Acute hematoma in a 19-year-old woman. The right capsule–thalamic hematoma is isointense on a T1-weighted (not shown), hypointense on a T2-weighted, and hypointense on a DW image with low ADC values.

C, Early subacute hematoma in a 54-year-old man. The right parietal lobe hematoma is hyperintense on a T1-weighted (not shown), hypointense on a T2-weighted, and hypointense on a DW image acquired with low ADC values.

D, Late subacute hematoma in a 73-year-old man. The right temporo-occipital hematoma is hyperintense on a T1-weighted (not shown), hyperintense on a T2-weighted, and hyperintense on a DW image acquired with low ADC values.

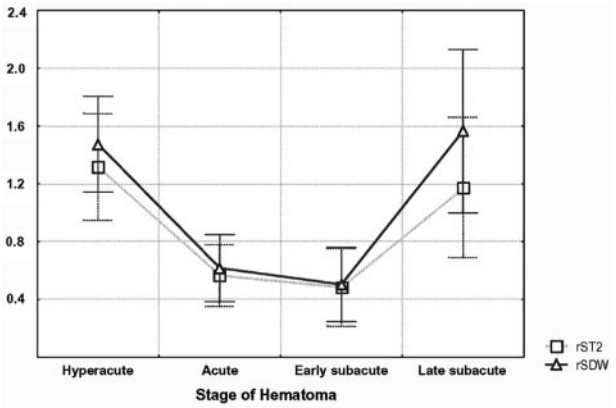

FIG 3. Signal intensity ratios according to the hematoma stages (mean ± SD). Throughout the course of the hematoma, the signal intensity ratio on DW (rS_{DW}) and on T2-weighted echo planar (rS_{T2}) images are positively correlated ($r = 0.93$, $P < .05$).

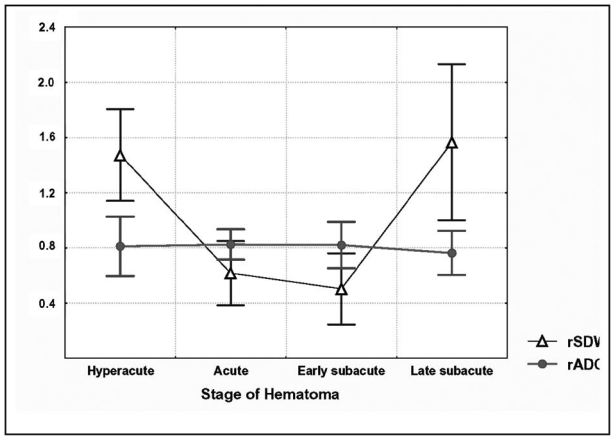

FIG 4. Signal intensity ratio on DW images (rS_{DW}) and ADC ratio (rADC) according to the stage of intracerebral hematomas (mean ± SD).

While rS_{DW} shows significant changes throughout the course of the hematoma, rADC values are moderately and significantly decreased throughout the course of hematoma ($P < .001$). No correlation is observed between rADC and rS_{DW} ($r = 0.09$, $P = .6$).

that restriction of diffusion is present in early intracranial hematomas without parenchymal infarction. Importantly, the reduction in ADC values that we observed did not significantly differ between the different stages of the hematomas. Such a steady decrease in ADC values would be expected to produce DW imaging hyperintensity, which should remain stable throughout the course of hematoma. The clear variation in DW imaging signal intensity according to the stage of the hematoma implies that factors other than ADC values influence the signal intensity on DW images. Indeed, DW imaging is not a simple map of diffusion motions but is a composite of contributions from diffusion and T1 and T2 effects. Because of these spillover effects, the DW images should be interpreted with reference to images obtained with other sequences, such as T2-weighted sequences and ADC maps. The term "T2-shine-through" has been coined to describe the substantial contribution of T2 hyperinstensities observed on DW images. First studied in ischemic stroke (19–21), this effect has since been described in a wide range of brain disorders (22). For hematomas, as expected, T2-hyperintense hematomas were also hyperintense on DW images, with a strong correlation between the signal intensity measured on T2-weighted and DW images. In contrast to hyperacute ischemic stroke, which lacks T2 signal intensity changes, the T2 shine-through effect in hyperacute hematoma seems to be an important component of the signal intensity on DW images. At the acute and early subacute stages, hematomas share the feature of hypointensity on T2-weighted images. These T2-hypointense hematomas were equally hypointense on DW images. The correlation we observed between the T2-weighted and DW image signal intensity in T2-hypointense hematomas suggests a contribution of the "T2 blackout effect," which is the corollary of the T2 shine-through effect.

Our study had some limitations. First, we chose to analyze globally the core of the hematoma, thus masking local signal intensity and ADC changes. This analysis was carried out on a single representative section, where the hematoma was the largest and the T2-hypointense ring most visible and thus most clearly distinguishable from the perihematoma. Although it could be argued that 3D region-of-interest analysis would have been more appropriate, our method minimizes the risk of partial volume effect with the perihematoma. Furthermore, our quantitative results corroborate our qualitative results, as well as other previous descriptive analyses. Second, to reduce the risk of computing erroneous ADC values for T2-hypointense hematomas, we did not mask for background noise. This could have potentially introduced some noise in ADC measurements. Using this method, the ADC values we computed for T2-hypointense hematomas were lower than those of Maldjian et al (17), who reported normal ADC values in a similar population of patients. Yet, normal ADC values add further evidence of the contribution of T2 blackout effect to the DW imaging signal intensity drop. Third, the respective contribution of proton density and T1 effect on DW imaging has not been addressed here. Proton density–weighted sequences were not part of the comprehensive stroke MR imaging protocol performed in most of our patients, and T1-weighted images were often obtained in the sagittal plane, hindering precise co-registration with axial DW images. T1 effects might not be a major component of DW imaging signal intensity. In particular, at the hyperacute stage, the hematoma is mainly isointense on T1-weighted images, and at the early subacute stage opposite signal intensity variations are usually observed on T1-weighted and DW images.

Conclusion

Our data, obtained by using gradient strengths with *b* values of 1000 s/mm^2, indicate that in the core of the hematoma: 1) ADC values are moderately but significantly decreased during the initial three stages of hematoma, without any significant variation throughout the course of the hematoma; 2) T2 shine-through

effects contribute to the signal intensity of hyperintense hematomas on DW images, and similarly, T2 blackout effects contribute to the signal intensity of hypointense hematomas on DW images. This extends to hematoma, the well-known principle that DW imaging signal intensity changes should be interpreted in light of the T2 signal intensity changes, especially at the earliest time point, when both hematoma and acute ischemic stroke are strikingly hyperintense on DW images. Improving our knowledge of the typical DW imaging–ADC patterns of primary hematoma could help in the diagnosis of secondary hematoma, which remains a challenging radiological problem.

References

1. Qureshi A, Tuhrim S, Broderick J, et al. **Spontaneous intracerebral hemorrhage.** *N Engl J Med* 2001;344:1450–1460
2. Linfante I, Llinas RH, Caplan LR, Warach S. **MRI features of intracerebral hemorrhage within 2 hours from symptom onset**. *Stroke* 1999;30:2263–2267
3. Patel MR, Edelman RR, Warach S. **Detection of hyperacute primary intraparenchymal hemorrhage by magnetic resonance imaging**. *Stroke* 1996;27:2321–2324
4. Schellinger PD, Jansen O, Fiebach JB, Hacke W, Sartor K. **A standardized MRI stroke protocol: comparison with CT in hyperacute intracerebral hemorrhage**. *Stroke* 1999;30:765–768
5. Fiebach JB, Schellinger PD, Gass A, et al. **Stroke magnetic resonance imaging is accurate in hyperacute intracerebral hemorrhage. A multicenter study on the validity of stroke imaging.** *Stroke* 2004;22:1–5
6. Gomori JM, Grossman RI, Goldberg HI, Zimmerman RA, Bilaniuk LT. **Intracranial hematomas: imaging by high-field MR**. *Radiology* 1985;157:87–93
7. Atlas SW, Thulborn KR. **MR detection of hyperacute parenchymal hemorrhage of the brain**. *AJNR Am J Neuroradiol* 1998;19:1471–1477
8. Bradley WJ. **MR appearance of hemorrhage in the brain**. *Radiology* 1993;189:15–26
9. Atlas S, Mark A, Grossman R, Gomori J. **Intracranial hemorrhage: gradient-echo MR imaging at 1.5 T. Comparison with spin-echo imaging and clinical applications.** *Radiology* 1988;168:803–807
10. Hackney D, Atlas S, Grossman R, et al. **Subacute intracranial hemorrhage: contribution of spin density to appearance on spin-echo MR images.** *Radiology* 1987;165:199–202
11. Hayman L, Taber K, Ford J, Bryan R. **Mechanisms of MR signal alteration by acute intracerebral blood: old concepts and new theories.** *AJNR Am J Neuroradiol* 1991;12:899–907
12. Clark R, Watanabe A, Bradley WJ, Roberts J. **Acute hematomas: effects of deoxygenation, hematocrit, and fibrin-clot formation and retraction on T2 shortening.** *Radiology* 1990;175:201–206
13. Atlas SW, DuBois P, Singer MB, Lu D. **Diffusion measurements in intracranial hematomas: implications for MR imaging of acute stroke**. *AJNR Am J Neuroradiol* 2000;21:1190–1194
14. Ebisu T, Tanaka C, Umeda M, Aoki In. **[Principles and clinical applications of diffusion weighted echo planar MR imaging]**. *Nippon Rinsho* 1997;55:1742–1747
15. Ebisu T, Tanaka C, Umeda M, et al. **Hemorrhagic and nonhemorrhagic stroke: diagnosis with diffusion-weighted and T2-weighted echo-planar MR imaging**. *Radiology* 1997;203:823–828
16. Kang BK, Na DG, Ryoo JW, et al. **Diffusion-weighted MR imaging of intracerebral hemorrhage**. *Korean J Radiol* 2001;2:183–191
17. Maldjian JA, Listerud J, Moonis G, Siddiqi F. **Computing diffusion rates in T2-dark hematomas and areas of low T2 signal**. *AJNR Am J Neuroradiol* 2001;22:112–118
18. Lin DD, Filippi CG, Steever AB, Zimmerman RD. **Detection of intracranial hemorrhage: comparison between gradient-echo images and b(0) images obtained from diffusion-weighted echo-planar sequences**. *AJNR Am J Neuroradiol* 2001;22:1275–1281
19. Burdette JH, Elster AD, Ricci PE. **Acute cerebral infarction: quantification of spin-density and T2 shine-through phenomena on diffusion-weighted MR images**. *Radiology* 1999;212:333–339
20. Warach S, Gaa J, Siewert B, Wielopolski P, Edelmann RR. **Acute human stroke studied by whole brain echo planar diffusion weighted magnetic resonance imaging**. *Ann Neurol* 1995;37:231–241
21. Knight R, Dereski M, Helpern J, Ordidge R, Chopp M. **Magnetic resonance imaging assessment of evolving focal cerebral ischemia. Comparison with histopathology in rats**. *Stroke* 1994;25:1252–1261
22. Stadnik T, Demaerel P, Luypaert R, et al. **Imaging tutorial: differential diagnosis of bright lesions on diffusion-weighted MR images.** *Radiographics* 2003;23:e7